Closed loop control of aerodynamic load fluctuations on wind turbine airfoil using surface plasma actuators

D. Nelson-Gruel, Pierric Joseph, Alexis Paulh-Manssens, Annie Leroy, Sandrine Aubrun-Sanches, Yann Chamaillard

Closed loop control of aerodynamic load fluctuations on wind turbine airfoil using surface plasma actuators

Dominique NELSON-GRUEL*, Pierrick JOSEPH, Alexis PAULH-MANSSENS*, Annie LEROY***, Sandrine AUBRUN****, Yann CHAMAILLARD***

** University of Orléans, INSA-CVL, PRISME, EA4229 - 8, rue Léonard de Vinci, 45072 Orléans, France France (Tel: +336-897-28280; e-mail: dominique.gruel-nelson@ univ-orleans.fr).*
*** Univ. Lille, ENSAM, FRE3723–LML–Laboratoire de Mecanique de Lille, F-59000, Lille, France (e-mail: pierric.joseph@ensam.eu).*
****French Air Force Academy Research Center, Base aérienne 701, 13661 Salon Air, France (e-mail: annie.leroy@ecole-air.fr)*
**LHEEA, Ecole Centrale de Nantes, UMR CNRS 6598, 44321 Nantes, France (e-mail: sandrine.aubrun@ec-nantes.fr).*

Abstract: In a century where the green energy is a vital challenge, research about wind turbine is taking its place to give an alternative solution to polluting and fossil energies. Various scales of studies are possible for wind turbine production and lifetime optimization, such as the farm, the wind turbine or the blade. In this study we focused on the alleviation of aerodynamic load fluctuations produced by airflow speed and incidence angle variations by means of active flow control. Wind turbine greatly loses its efficiency when faced to wind gusts, moreover, the blade life span is reduced by the load oscillations created by wind disturbances. Thus, a control technic based on a surface plasma actuator is studied to reduce lift oscillation and actively keep a constant lift. Plasma actuator is used to manipulate the air circulation around the blade, thus, the lift. Proofs of concepts are conducted thanks to experiments in a wind tunnel and through numerical modelling.

Keywords: Wind turbine airfoil, Surface plasma actuator, Circulation control, Disturbance rejection, loop-shaping controller.

1. INTRODUCTION

Energies are one of the most challenging issues of modern societies. Both the fossil resources reduction and the increasing pollutant emissions bring the question of alternative energy sources. Since the beginning of the 21st century, renewable energy has become more present around the world. At the end of 2016, they represent up to 24% of the global electricity production. These 24% represent different renewable sources as hydropower (16%), wind power (4%), solar power (1.5%) and others. Due to its least levelized cost of electricity compare to other green energies, wind energy is a competitive solution to meet societies' queries (Janet *et al* (2017)).

Today, wind energy represents a world production near 500 Gigawatts with China, United-States and Germany as leaders. However, the electric production is optimized when the turbine has a constant rotational speed. Thus, wind turbines would need a constant airflow speed and direction to meet this requirement. Obviously, it is not possible to have a constant wind. Atmospheric boundary layer provokes inhomogeneous and unsteady wind as gusts or turbulences. The appearance speed of these effects, Burton *et al* (2002), being too fast for a pitch angle control, both the rotational speed and the aerodynamic loads applied on the blades vary significantly. Hence, both turbines efficiency and sustainability are reduced.

Lot of research have been conducted to modify the air flow around airfoils and reduce these effects as presented in Herbert *et al* (2007), Barlas *et al* (2010) and Aubrun *et al* (2017). Although passive actuation (as trailing edge flaps) may give good results for some operating point, it can produce losses in other. Thus, active actuation (as plasma or fluidic jets) offers a good perspective for this purpose. The work presented in this article is part of the project Smart Rotors to Improve Wind Energy Efficiency and Sustainability (Smarteole) supported by the French "Agence Nationale de la Recherche" (ANR). It aims at reducing the aerodynamic load fluctuations and the blade fatigue to increase the rotor efficiency and lifetime using active actuations like Plasma or fluidic actuators. The present study deals with overload reduction at the blade scale and is experimented in a wind-tunnel (Fig.1). This article presented a proof of concept for the use of Plasma actuations to reduced aerodynamic load fluctuations.

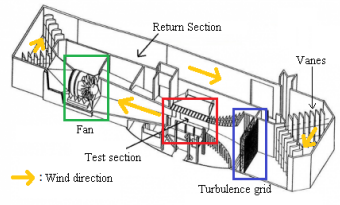

Fig. 1: Large subsonic wind tunnel diagram (PRISME Laboratory).

In this document, section 2 will be dedicated to the presentation of the experimental setup. In section 3 the used identification process will be described and section 4 and 5 will deal with the design and assessment of the control law that enables load fluctuation reduction.

2. EXPERIMENTAL SET-UP

Air instability and natural or artificial landscape obstacles may induce wind gusts. These incoming wind variations may provoke high load fluctuations on the rotor (Rezaeiha *et al*, (2017)), thus, reduce the efficiency and rotor lifespan. In response to these wind variations (in intensity and direction), most horizontal axis wind turbines (HAWT) use pitch control. However, this acts on the whole blade and has a longer time-response than wind gust occurrence time. Thus, active flow control technics (flaps, microtabs, fluidic devices…), as presented in Cattafesta *et al* (2011), make sense to obtain fast and modular flow control on the rotor blades.

Fig. 2 represents the effect of a gust angle variation on the lift versus the angle of attack airfoil curve. When the wind disturbance occurs, the objective of the control will be to keep the lift at a constant value.

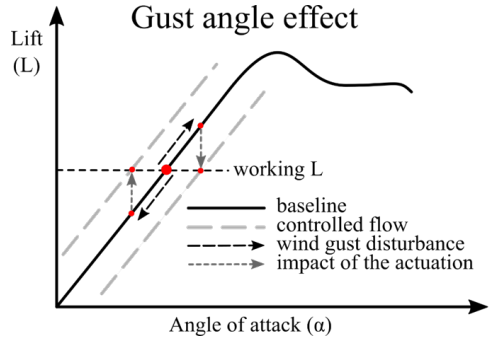

Fig. 2: Gust angle effect on the lift.

Because experiments are performed at the wind tunnel scale (Fig. 1), wind gusts must be modelled in accordance. Thus, it is necessary to have referential values to denote what should be the system characteristic time. In aerodynamics, the chord time is commonly used:

$$Tc = \frac{C}{U_\infty}, \qquad (1)$$

where C is the chord of the blade airfoil [m] and U_∞ the freestream fluid velocity [m/s]. This value represents the time for an air particle to travel from the leading to the trailing edge of the airfoil and permits a comparison between different systems with different shapes. The interesting values in our application are the characteristic time of flow response establishment ($10*Tc$) and the characteristic time of an aerodynamic disturbance ($100*Tc$). In our case, it has been defined that the aerodynamic disturbance time is about 3s.

In order to have a representative model of a gust angle variation, it has been chosen to impose an oscillation of the blade angle of attack. This variation is a sinusoidal movement with a 1° amplitude and about 1/3 Hz frequency.

2.2 Blade configuration in the wind tunnel

Experiments in the wind tunnel main test section have been conducted reproducing a two-dimensional translational flow conditions, i.e. the airfoil was horizontally mounted and attached to each tip as presented in Fig.3. Surface plasma actuators have been mounted on a NACA654-421 blade airfoil with a rounded trailing-edge (Fig.4). More details of this experimental set-up can be found in Baleriola *et al* (2016). In these experiments the incoming flow velocity was fixed at 10m/s, the wing span and the chord are 1.1 [m] and 0.3 [m] long respectively

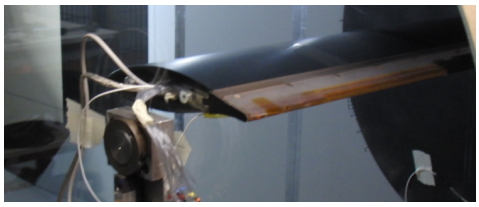

Fig. 3: Picture of the bidimensional configuration of the blade.

In order to obtain measurements, the blade was mounted on a 6-component platform balance. 20 pressure taps were distributed around the airfoil and Particle Image Velocimetry (PIV) could be used for some experiments. The pressure taps are used to obtain the pressure distribution around the blade, therefore the lift by integration (Fig. 4). A precise scale sensor is used to validate the Lift value obtain by the low-cost pressure sensors.

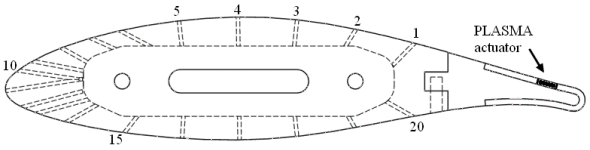

Fig. 4: Sectional view of the blade with pressure tap locations

2.3 Actuators and their implementation on the blade

The plasma actuator was placed at the trailing edge to produce an airflow near the end of the blade. Thus, air circulation can be slightly modified inducing lift variation.

The plasma actuator used in this work is based on a Dielectric Barrier Discharge (DBD) (Fig. 5 & Fig. 6), . It consists of two electrodes separated by a dielectric layer (Corke *et al*, (2010))). Supplying the upper electrode exposed to the air by an alternative high voltage, it can ionize the surrounding air inducing an airflow named ionic wind (about 5 m/s for the actuators used in this project). This plasma-induced flow can be used for circulation control strategy (Joslin & Jones, (2006)) around a wind turbine blade in order to increase or decrease the lift (Baleriola *et al* (2016)).

The way the actuator is mounted on the blade only allows downward jets, thus, it is only possible to increase the lift.

This kind of active flow control has lot of advantages for industrial applications. First of all, there is no moving part and

the implementation of such device does not need to modify the structure of the receiving system. Moreover, its low weight and fast time response allow it to be studied in high-G applications (Shyy *et al* (2002), Suzen *et al* (2005), Corke *et al* (2010) and Likhanskii *et al* (2010)). Main disadvantages are its limited velocity output and it requires a high voltage causing some electromagnetic disturbances.

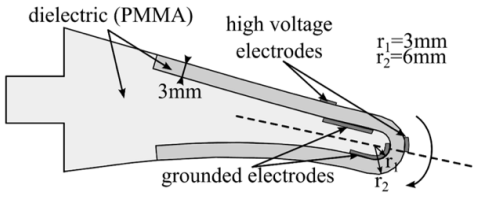

Fig. 5: Sectional view of the airfoil trailing edge.

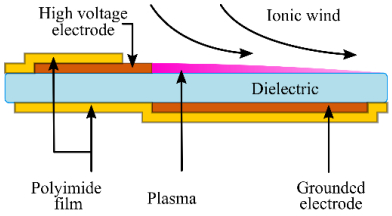

Fig. 6: DBD diagram.

The high voltage electrode is supplied by an AC-power supply up to 20kV for a typical power consumption around 40W/m. The variable to control this system is therefore the voltage provided by the low frequency generator from 0 to 2.5 Volts (U_{gbf}) which operates the high voltage power supply

3. SYSTEM IDENTIFICATION AND ANALYSIS

Numerous studies have been done both experimentally and numerically to understand and compute the behavior of the device. As a first modelling approach, the work of Shyy *et al* (2002) proposed an analytical approach to implement the DBD in the Navier-Stokes equations as a body force, supposing the electric field as linear. However, this simplified phenomenological model can lead to infinite values as the frequency and voltage increase. Suzen *et al* (2005) gave a more precise mathematical model again with an application for Reynolds Averaged Navier-Stokes (RANS) CFD computations by making different hypothesis for the electric field. However, studies of viscous effects on the DBD shows that up to 70% of the induced thrust is lost due to the drag. Although it is possible to add plasma influence on CFD computations, it is not yet so straightforward to obtain dynamic models . Thus, it has been chosen to use experimental database to create a black-box model of the system.

3.1 System Definition

The representative variable of the system is the lift coefficient (C_L). On our blade, multiple pressure sensors are placed to obtain the pressure repartition around the blade (numbers 1 to 20 – Fig. 4). The integration of these pressures makes possible the computation of the lift and the corresponding non-dimensionalized lift coefficient.

$$L = \oint pn \cdot k \, dS, \qquad (2)$$

$$C_L = \frac{2L}{\rho U_\infty^2 S}, \qquad (3)$$

where L is the lift force [N], S the surface of the airfoil [m^2], p the pressure [Pa] around the airfoil, n the normal unit vector pointing into the blade, k the vertical unit vector normal to the freestream direction, ρ the fluid density [kg/m^3], and U_∞ the flow speed [m/s].

From an industrial point of view, it is not relevant to distribute pressure taps all around the blade due to a complex manufacturing. Then, it has been chosen to work with one pressure tap and measure the pressure coefficient for comparison:

$$C_p = \frac{P - P_\infty}{0.5 \rho U_\infty^2}, \qquad (4)$$

where P is the evaluated static pressure [Pa], P_∞ is the pressure in the freestream [Pa], ρ is the freestream fluid density (1.225 at sea level and 15°C) [kg/m^3], U_∞ is the freestream fluid velocity [m/s].

Although the lift cannot be computed thanks to only one pressure tap, it can be approximated for little angle of attack variation. To obtain relevant results, the tap with the greatest amplitude variation in the working conditions was chosen; the tap number 10 in the vicinity of the leading edge (Fig. 7). Consequently, in this experiment, the freestream is constant (about 10m/s), the angle of attack oscillation is used for gust modeling and the DBD actuator is the command in V, U_{gbf}. This command is linearly linked to the plasma actuator voltage, U_{PL} in kV. The lift is measured precisely with a scale sensor but must be estimated thanks to the pressure sensor at tap 10.

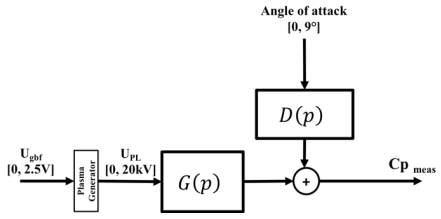

Fig. 7: System diagram.

As first hypothesis, we supposed that the superposition theorem could be used to identify the system. In other words, we supposed that the effects of AoA and DBD could be studied separately for some operating points.

3.2 Static Analysis

The available data gave different outputs for unitary variation of AoA and for different applied voltages to the DBD. The cartography is computed looking at the steady state values for all different operating points and averaged from different tests. With AoA going from 3 to 9 degrees and voltage input equal to 0, 15, 17 and 19 kV, 28 values are then obtained. Because of a small amount of test points, a mathematical study has been performed thanks to the software XFoil in order to understand the behavior between these steady state points. This study has

shown that, for AoA between -5° and 10°, the pressure evolution at tap 10 can be approximated by a polynomial form of second order.

Hence, with seven points for AoA values between 3° and 9°, and knowing the theoretical shape, an approximation of this curve can be computed. This allow a better understanding and assessment for the inter-point behavior (Fig. 8).

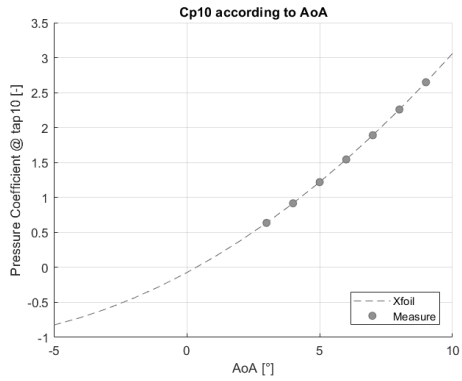

Fig. 8: Pressure coefficient at tap10 according to AoA.

3.3. Dynamic identification

The frequency-domain control-system-design (CSD) approach used in this work requires high fidelity linear dynamic models that approximate the underlying dynamics of the system. Thus, a frequency domain system identification methodology was used to obtain a linear time-invariant model that approximates the dynamics of the airfoil around one operating point defined by plasma voltage and angle of attack values. It must be noticed that the sensor that gives the lift coefficient or force couldn't be used to developed the control algorithm but only to assess this one in terms of gains. To identify the system, some step signals on inputs (U_{PL} and α) were used. The identification process of the dynamic is separated in two main steps.

Using pressure tap, plasma signals, angle of attack and Fast Fourier Transform (FFT) algorithm, the frequency response and the input-output transfer function of the system are found, $G(p)$. This process is repeated for all operating points cited in section 3.2. Fig. 9 shows some step responses of the plasma voltage variations.

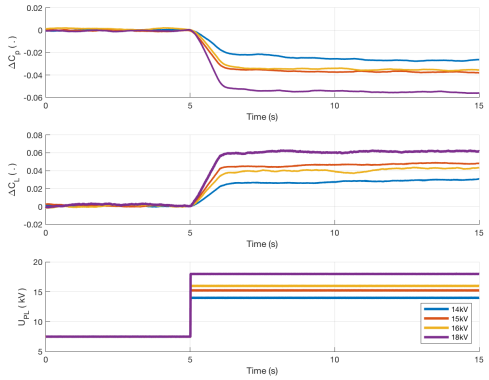

Fig. 9: Experimental results of step response of plasma voltage.

The frequency domain identification provides a parametric model that approximates the system at each operating point by a linear time-delay transfer function (Fig.10). The second identification step consists in searching the transfer function between the perturbation signal and the output signal. To do this, some other step responses for the angle of attack are realised for fixed values of plasma signal (Fig. 11).

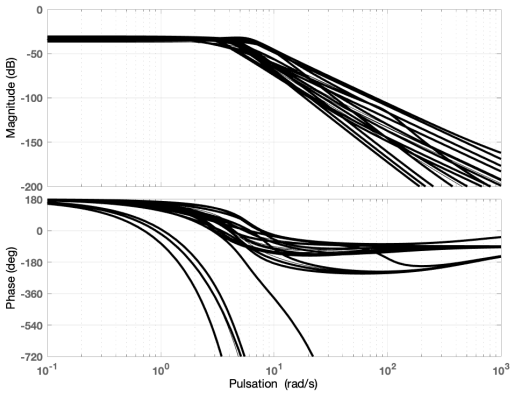

Fig.10: Bode diagram of the identified system $G(p)$ around twenty operating points.

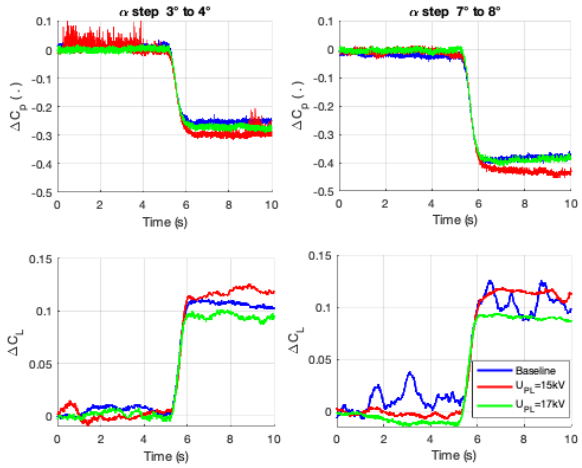

Fig. 11: Experimental results of step response of angle of attacks for various plasma signals

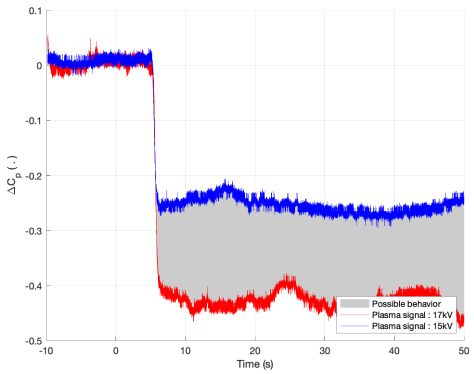

Fig.12: Pressure coefficient response to various angle of attacks and plasma voltages.

Fig. 12 shows the possible variation of the relative pressure coefficient under all possible variations of angle of attacks and plasma voltages. These time-response curves are used to found the frequency response and the transfer function that correspond to the perturbation part of the system (Fig. 13).

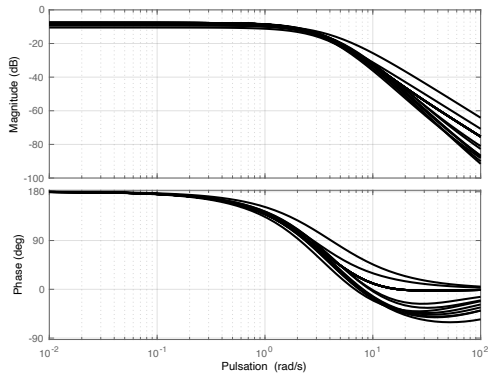

Fig.13: Bode diagram identification results of the system around twenty operating points.

Finally, with all defined variables, the model is assessed using real measurement. Fig. 14shows a series of AoA steps (of 1° amplitude from 3° to 9°) for a given actuation of plasma (the applied voltage is fixed at 15kV in this case), inducing a C_L variation.

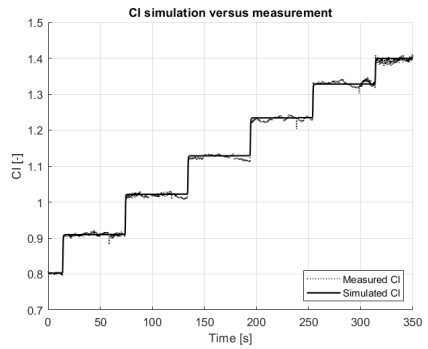

Fig. 14: C_L simulation versus measurement.

4. CONTROL SYSTEM DESIGN BY LOOP-SHAPING

The control strategies proposed in this section uses loop-shaping control methodology, in which optimisation is used to find the controller that satisfies the control specification. The aim of the control law is to reduce the load fluctuations. The loop-shaping used in this work is based on the common unity-feedback configuration, Fig. 14. The transfer function $K(p)$ is parameterized to satisfy the three following objectives:

- Time response for the nominal plant lower than 3 seconds,
- Perfect accuracy at low frequencies,
- Perfect disturbance rejection for the nominal plant with a time rejection lower than 3 seconds.

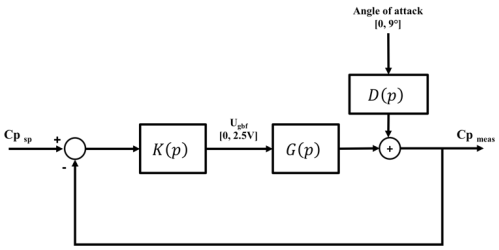

Fig.14: Control-system diagram.

Fig. 15 and Fig. 16 show the nominal and re-parametered magnitude of the complementary sensitivity and sensitivity transfer function respectively. These two figures and the measurement of the maximum amplitude of the complementary sensitivity function, as well as the cut-off frequencies, validate the three objectives of the specifications.

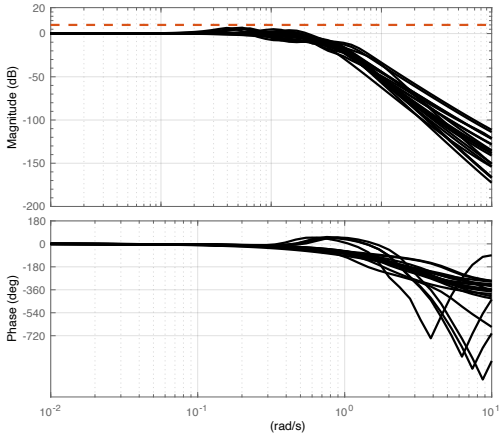

Fig.15: Bode diagram of T and highest value of the resonant peak of each complementary sensitivity functions (red dash-line).

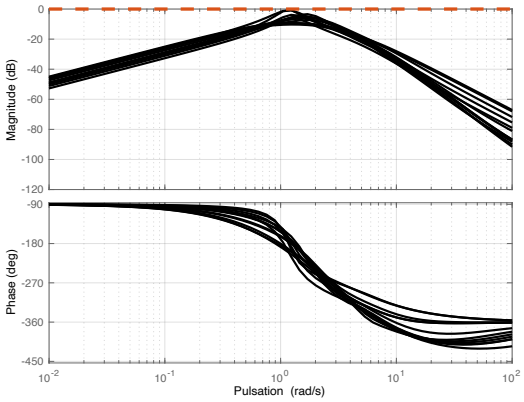

Fig.16: Bode diagram of S and highest value of the resonant peak of each sensitivity functions (red dash- line).

5. RESULTS AND DISCUSSIONS

5.1. Preliminary test

The designed controller has been assessed with some time-domain tests on the wind tunnel set-up. As a preliminary step, the control-loop is tested with a constant set point and a simple scheme of perturbation (step variation of the angle of attack).

Due to mechanical constraint (weight of the model and fragility of the aerodynamic balance), step motion takes nearly 1 s to be realized. It is quite long compare to the characteristic time of the system, but it remains comparable to the timescale of the natural wind (see section 2.1). Fig. 17 presents the pressure coefficient measured with regulation (red curve), compared with baseline (blue curve).

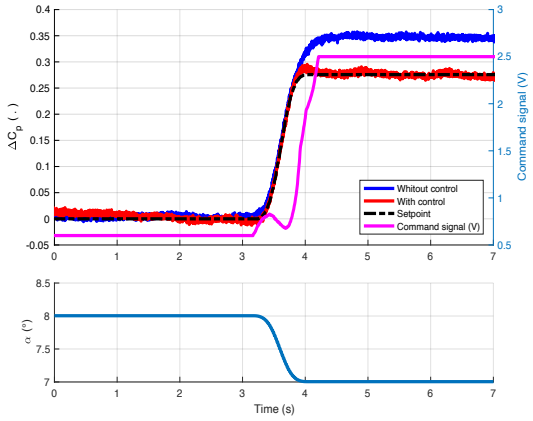

Fig.17: Angle of attack variation for preliminary control test and experimental results.

This test proves the viability of the whole regulation concept with DBD actuator applied for circulation control. An additional test is performed at a fixed angle of attack ($\alpha = 4°$), and the controller is suddenly deactivated (slightly after $t \approx 4{,}5$ s, see Fig. 18). Once control is deactivated, pressure coefficient at the tap #10 slowly recovers its uncontrolled state. Recovery time is close to 0.6 s, which is an interesting result from an aerodynamic point of view. It corresponds to $20Tc$, which is in agreement with classical results on canonical geometry (Darabi *et al* (2004)) meanwhile being detached flows.

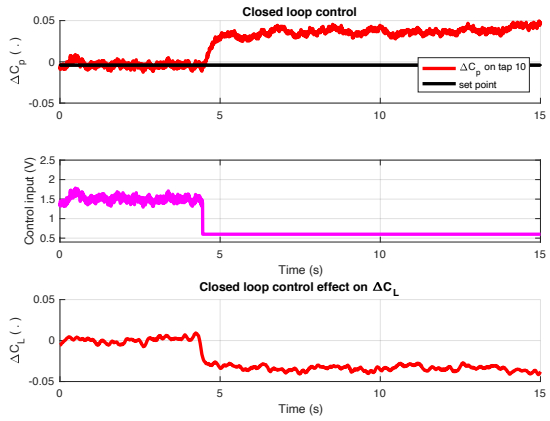

Fig.18: Preliminary test results – control deactivation.

5.2. Sine response

The relative simplicity in the sensor choice (only one pressure tap) leads to some complexity in the set point design. In fact, a particular level of pressure in the chosen pressure tap can be associated to different situations: measurement can be similar for a configuration with a certain angle of attack and for another configuration with a smaller angle of attack but with actuation activated. Clearly speaking, one cannot associate simply a pressure level in pressure tap #10 to a certain level of lift. A more complex set point is then required. Another difficulty lies in the fact that the DBD actuator chosen for the experiments can only increase the lift. Considering the characteristics of the perturbation discussed in Section 2.1, one also needs to deal with phases where regulation will not be necessary.

To address these concerns, the set point definition must include partially the measurement of the angle of attack in the regulation loop. It will not be used as an entry of the controller, but as an activating condition (see the explicative scheme in Fig. 19).

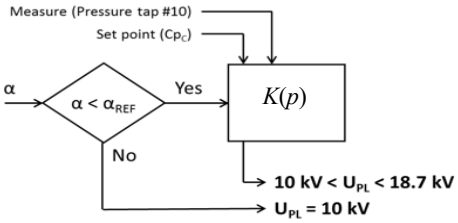

Fig.19: Schematic description of the set point.

The idea behind this definition is to build a smooth trajectory for the set point when the angle of attack begins to decrease in order to reach maximum correction for the minimal α value.

The system is submitted to a periodic variation of the angle of attack as defined in section 2.1. Time series are provided on Fig. 20. Control is activated simultaneously at the beginning of the test. Fig. 20 presents the effects observed on the pressure #10 used as sensor for this regulation test. As for preliminary test, uncontrolled baseline is in blue, while regulated pressure is depicted in red. First observation is that the effect of the regulation is clearly visible for the high pressures (respectively minimal angles of attack), meanwhile being unchanged for the low pressures (high angles of attack). Second observation is that set point trajectory is slightly shifted compared with both baseline and controlled cases. This is unexpected but it could be linked to the internal delay due to the whole system. In fact, set point trajectory is intended to be a perfect image of the pressure for a given value of AoA. But the "true" value is gathered by the sensor with a certain delay, plus the delay needs to perform α variation. Lift increase is asymmetrical (compare with baseline), due to the delay of the command rise. Despite this delay, a 16% reduction of the fluctuation is achieved considering pressure coefficient and 5% considering lift coefficient.

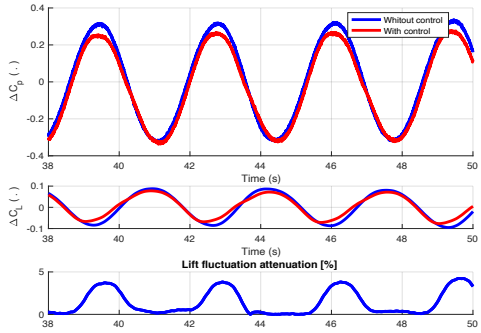

Fig.20: Sine response – effect on the lift coefficient.

6. CONCLUSION

The present study deals with lift regulation of a wind turbine airfoil. Main goal is to alleviate load fluctuations in order to prevent fatigue effect on the blades. A reduced scale airfoil with a modified trailing edge is studied in wind tunnel in a 2D configuration. Lift is manipulated through circulation control strategy (modification of the Kutta's condition at the trailing edge) using surface plasma actuators (DBD).

In order to stick with industrial constraints, one single pressure tap is used as a sensor to drive the controller. Open loop tests reveal that leading edge taps are promising in that role, due to high level of pressure at this location. Identification also indicated that the SISO system composed by this tap and the supply voltage of the DBD actuator is piecewise linear. Thanks to this linearity, a simple loop-shaping methodology has been used to design a controller that regulates the pressure coefficient and so the lift force.

Preliminary tests are performed studying step response. Then, the control law has been assessed using a disturbance rejection test (sinusoidal variation of the angle of attack). Despite a sub optimal set point tracking, the controller provides up to 16% of reduction of load fluctuations.

These encouraging results call for some improvements of the current setup. Set point design has to be modified to take into account the internal delay of the measurement devices. Controller could be improved with more sophisticated regulation methods like robust control or predictive control.

In the aim to go toward industrial applications, an important milestone would be to achieve both lift decreasing and lift increasing, and also to test such control strategy on advanced test bench like a reduced scale wind turbine.

7. ACKNOWLEDGEMENT

Funding: This work was supported by the French national project SMARTEOLE (ANR-14-CE05-0034).

REFERENCES

Aubrun, S., Leroy, A. & Devinant, P. (2017) A review of wind turbine–oriented active flow control strategies. *Experiments in Fluids*, p.19.

Baleriola, S., Leroy, A., Loyer, S., Devinant, Ph., Aubrun, S. (2016) Circulation control on a rounded trailing-edge wind turbine airfoil using plasma actuators. *Journal of Physics: Conference Series*, 753(5), p.52001.

Baleriola, S., Leroy, A., Loyer, S., Devinant, Ph., Aubrun, S. (2018) Experimental lift control using fluidic jets on a model wind turbine. *Journal of Physics: Conference Series*, 753(5), p.52001.

Barlas TK and van Kuik GAM (2010) Review of state of the art in smart rotor control research for wind turbines. Prog Aerosp Sci 46(1):1–27

Burton T, Sharpe D, Jenkins N, Bossanyi E (2001) Wind Energy Handbook. John Wiley & Sons, Chichester.

Cattafesta, L. & Sheplak (2011) M., *Actuators for active flow control*, Annual Review Fluid Mechanics 43:247–72.

Corke, T. C., Enloe, C. L., & Wilkinson, S. P. (2010). Dielectric barrier discharge plasma actuators for flow control. Annual review of fluid mechanics, 42, 505-529.

Darabi, A. & Wygnanski, I., 2004. Active management of naturally separated flow over a solid surface. Part 1. The forced reattachment process. *Journal of Fluid Mechanics*, 510, pp.105–129.

Herbert, G., Iniyan, S., Sreevalsan, E., Rajapandian, S.. (2007). A review of wind energy technologies. *Renew Sustain Energy Rev. Renewable and Sustainable Energy Reviews.* 11.

Jaunet, Vincent & Braud, Caroline. (2018). Experiments on lift dynamics and feedback control of a wind turbine blade section. *Renewable Energy.* 126.

Joseph, P., Nelson-Gruel, D., Leroy, A., Baleriola, S., Aubrun, S., Haidous, Y., Loyer, S., Devinant, Ph..(2017) Circulation control using surface plasma actuators for aerodynamic load alleviation on wind turbine airfoils, *23ème Congrès Français de Mécanique.*

Joslin, R., Jones, G.. (2006) *Applications of circulation control technology*, AIAA

Likhanskii, A.. (2010) Limitation of the DBD effects on the external Flow, AIAA 2010-470.

Janet, S. *et al*. (2017) Renewables 2017 Global Status Report, ISBN 978-3-9818107-6-9.

Rezaeiha A., Pereira R., and M. Kotsonis M. (2017) Fluctuations of angle of attack and lift coefficient and the resultant fatigue loads for a large horizontal axis wind turbine. Renewable Energy, 114:904-916.

Shyy, W., Jayaraman, B., Andersson, A.. (2003). Modeling of glow discharge-induced fluid dynamics. *Journal of Applied Physics.* 92(11). 6434 - 6443.

Suzen, Y., Huang, P., Jacob, Jamey, Ashpis, D.. (2005). Numerical Simulations of Plasma Based Flow Control Applications. *35th AIAA Fluid Dynamics Conference and Exhibit*.